J. Dairy Sci. TBC
https://doi.org/10.3168/jds.2025-26950
Published by Elsevier Inc. on behalf of the American Dairy Science Association®.

Exploring influenza A virus receptor distribution in the lactating mammary gland of domesticated livestock and in human breast tissue

Rahul K. Nelli,[1]*† Tyler A. Harm,[1]† Bailey Arruda,[2]† Chris Siepker,[1]† Olufemi Fasina,[1] Jennifer M. Groeltz-Thrush,[1] Amy Baker,[2] Rachel Phillips,[1] Brianna Jones,[1] Virginia Espina,[3] Hannah Seger,[2,4] Manoj Kumar,[1] Qamar Ul Hassan,[1] Gulnara Brixius,[1] C. Joaquin Caceres,[1] Silvia Carnaccini,[1] Luis Gimenez-Lirola,[1] Paul J. Plummer,[1] and Todd M. Bell[1]*†

[1]Iowa State University College of Veterinary Medicine, Ames, IA 50011
[2]Virus and Prion Research Unit, National Animal Disease Center, Agricultural Research Service, United States Department of Agriculture, Ames, IA 50010
[3]Center for Applied Proteomics and Molecular Medicine, School of Systems Biology, George Mason University, Manassas, VA 20110
[4]Oak Ridge Institute for Science and Education, Oak Ridge, TN, 37830

ABSTRACT

The spread of the highly pathogenic avian influenza (HPAI) H5N1 virus in dairy cattle, particularly affecting the mammary glands, highlights the adaptability of influenza A viruses (IAV) to infect nontraditional species. Mammals like pigs, sheep, goats, and camelids contribute >$30 billion annually to the US economy and are a source of meat and milk for millions, highlighting the importance of understanding viral susceptibility in these species. The zoonotic transmission of HPAI H5N1 to several dairy and poultry farm workers involved with farm operations during outbreaks is also a cause for public health concerns. Previous studies showed IAV-specific sialic acid (SA) receptors in the mammary glands of dairy cattle, but those studies did not explore their presence in pigs, sheep, goats, alpacas, and humans. The current study used lectin histochemistry staining with fluorescently labeled *Sambucus nigra* (SA α2,6-galactose [gal] receptors) and *Maackia amurensis* (SA α2,3-gal receptors) and found that the mammary glands of all of these species, including human breast, were rich in SA α2,6-gal receptors essential for mammalian-adapted IAV binding. We also found SA α2,3-gal receptors in the examined tissues of all species, although to a lesser extent. Notably, an A(H5N1) clade 2.3.4.4b virus demonstrated binding to both ruminant (cattle) and nonruminant (pigs) species' mammary tissue. These findings provide crucial insights into the potential for HPAI H5N1 to infect and spread within the mammary glands of these production animals, as well as humans.

Key words: sialic acid, α2,3-gal, α2,6-gal, H5N1, mammary gland, cattle, alpaca, sheep, goat, pig, human

INTRODUCTION

Since the first human case of highly pathogenic avian influenza (**HPAI**) H5N1 was reported in 1997, there has been limited evidence to suggest human-to-human transmission. With spillover from birds to humans, there have been years in which the peak annual human cases worldwide reached <150 (Tran et al., 2004; Shu et al., 2006; Le et al., 2019; CDC, 2025c). The case fatality ratios were close to 50%, raising serious public health concerns, albeit with low overall reported case numbers (Shu et al., 2006; Le et al., 2019; WHO, 2024). Interestingly, the current outbreak of HPAI H5N1 in dairy cattle and poultry in the United States has resulted in numerous spillovers into farm workers handling HPAI H5N1-affected dairy herds and poultry flocks. As of March 7, 2025, there have been 70 cases confirmed by the US Centers for Disease Control and Prevention, with one reported death associated with HPAI H5N1 (Mellis et al., 2024; CDC, 2025a). Influenza A viruses are known to replicate well in the respiratory and intestinal tracts of animals and humans (Uiprasertkul et al., 2005; Naguib et al., 2023). However, the continued HPAI H5N1 viral replication in the mammary gland of novel species like dairy cattle (Baker et al., 2025; Halwe et al., 2025a) with a combination of continued spillover into numerous naive mammalian species (USDA-APHIS Wildlife Services, 2025) raises the concern of HPAI H5N1 virus adaptation to mammalian species, with a possibility of continued mammal-to-mammal and even human-to-human spread.

To assess the current feasibility of HPAI H5N1 viral replication within the mammary glands of other exposed animals, this study aimed to delineate the spatial distribu-

Received May 16, 2025.
Accepted October 28, 2025.
*Corresponding authors: rknelli@iastate.edu and toddbell@iastate.edu
†These authors contributed equally to this work.

The list of standard abbreviations for JDS is available at adsa.org/jds-abbreviations-25. Nonstandard abbreviations are available in the Notes.

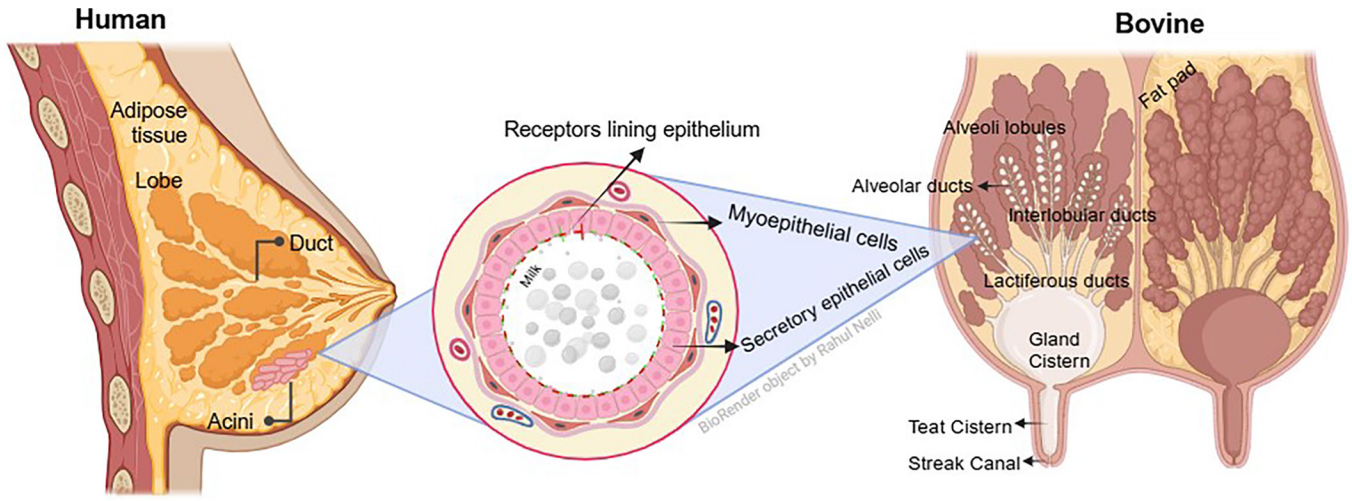

Figure 1. Illustration of sagittal section anatomy of the mammary gland of a cow. Inset image shows the microscopic anatomy of alveolar lobules with secretory epithelial cells, myoepithelial cells, and milk secretions.

tion of influenza A virus (**IAV**)-specific sialic acid (**SA**) receptors in the mammary glands of various production animals (pigs, sheep, goats, cattle, and alpacas) in comparison to human breast tissue. Due to recent spillovers from production animals into people, this study also examined human breast tissue.

The mammary gland's structure is complex and consists of a network of alveolar lobules interconnected by ducts and supported by connective, adipose, and smooth muscle tissues (Figure 1).

Pathogens, such as bacteria, viruses, and fungi, can invade the mammary gland and cause mastitis, a painful and debilitating condition. Interestingly, retrograde infection is the most common route or method of infection, where microorganisms enter through the teat opening and into the canal and cistern (Haxhiaj et al., 2022). The infection can spread to other animals through contaminated equipment or by direct contact, posing a significant threat to the health of an entire herd (Wieland, 2024).

A key factor in the susceptibility to HPAI H5N1 infection is the presence of specific host cell receptors that the virus uses for entry (Matrosovich et al., 1999). Influenza A viruses utilize host SA for initial attachment and cell entry (Matrosovich et al., 2013). Influenza A viruses exhibit host-specific receptor binding preferences based on the linkage type of SA to galactose. Mammalian-adapted strains preferentially bind to SA linked via an α2,6-galactose (**Gal**) or N-acetylgalactosamine (**GalNAc**), whereas avian-adapted strains favor SA linked via an α2,3-β-galactose (**α2,3-Galβ**; Kuchipudi et al., 2021). This distinction in receptor specificity is a key determinant of viral tropism and cross-species transmission potential.

Sialic acids are also potential receptors or co-receptors for other viral families such as *Coronaviridae* (Nguyen et al., 2022), *Paramyxoviridae*, *Flaviviridae* (Tan et al., 2019), *Picornaviridae* (Taube et al., 2009), *Reoviridae* (Haselhorst et al., 2009), *Parvoviridae* (Huang et al., 2016), *Adenoviridae* (Arnberg et al., 2000), *Papillomaviridae* (Zhang et al., 2024), *Polyomaviridae* (O'Hara et al., 2014), and *Caliciviridae* (Stuart and Brown, 2007). In addition, many bacteria, fungi, and parasites exploit SA as growth substrates for immune evasion, host cell entry, and enhanced virulence, including those that cause mastitis, such as *Escherichia coli*, *Streptococcus* sps., *Pasteurella* sps., *Candida* sps., *Aspergillus fumigatus*, *Leishmania*, and *Trypanosomes* (Warwas et al., 2007; Hopkins et al., 2013; Cavalcante et al., 2021; Eneva et al., 2021; Rifatbegović et al., 2024).

Sialic acids are a diverse group of 9-carbon carboxylated monosaccharides synthesized in animal species (Ghosh, 2020; Lewis et al., 2022). Sialic acids are also one of the major components of milk and play an important role in human nutrition, particularly in brain development (Wang and Brand-Miller, 2003; Sharma et al., 2019). Cattle and goat milk predominantly contain SA in the form of N-glycolylneuraminic acid versus N-acetylneuraminic acid, and their content decreases with the progression of the lactation stage (Puente and Hueso, 1993; de Sousa et al., 2015). In addition, SA levels vary depending on the diet of the animal and have been shown to regulate the microbiota-gut-mammary axis during mastitis in Holstein cows (Zhao et al., 2023). N-acetylneuraminic acid is also one of the key metabolites to be elevated in metastatic breast tumors in humans (Teoh et al., 2018). This suggests that SA levels may vary depend-

ing on the lactational stage, diet, and underlying disease conditions.

Understanding SA interactions within complex organs such as the mammary gland of production animals during lactation is essential. These interactions may influence host-pathogen dynamics, immune modulation, and milk composition, all of which are critical for animal health and productivity during this physiologically demanding stage.

MATERIALS AND METHODS

Sample Collection

The Institutional Animal Care and Use Committee of the Iowa State University (**ISU**) College of Veterinary Medicine (Ames, IA; IACUC-24-090) approved this study. We procured 3 animals of each species studied from the Iowa State University Research farms (sheep, goats, and beef cattle), or from approved vendors (alpacas). All lactating animals used in this study were actively lactating at the time of tissue collection. The animals were as follows: sheep (Polypay composite, 2–6 lactations), goats (American alpine, 2–6 freshenings/lactations), alpaca (2–8 cria/lactations), beef cattle (Simmental/Angus, 5–9 yr old), nonlactating heifer calves (Holstein × Angus crosses, 14 to 16 wk age), Holstein dairy cattle (multiparous), and pigs (parity 2 or greater). Following euthanasia, formalin-fixed and paraffin-embedded sections of the mammary gland from the area of the teat cistern, gland cistern, interlobular (collecting) duct, and secretory alveoli (glandular epithelium) were collected from these animals (Figure 2). In the case of the human mammary gland (nonlactating), we procured normal control breast tissue slides from a commercial vendor (Mopec, Madison Heights, MI; catalog no. SC936), and George Mason University (**GMU**) provided de-identified, formalin-fixed paraffin-embedded archived breast tissues collected with informed consent and Institutional Review Board approval (GMU IRB# 478170 and 477703). We obtained archived tissue blocks after consultation and approval from ISU and GMU.

Lectin Histochemistry

We characterized mammary tissues for SA using a lectin histochemistry assay as previously described (Nelli et al., 2024) for chromogenic and fluorescent staining. Briefly, we sectioned formalin-fixed, paraffin-embedded mammary gland tissue sections at 4 µm with placement on Superfrost Plus slides (VWR International). After drying the slides at 60°C for 20 min, we performed deparaffinization and staining on the Roche Diagnostics Ventana DISCOVERY ULTRA research platform. We retrieved the heat-induced epitope using Cell Conditioning CC1 solution at 100°C for 24 min (Roche Diagnostics Corporation). Endogenous peroxidase was quenched for chromogenic staining using Discovery Inhibitor (Roche Diagnostics Corporation). Slides were then blocked with 1× Carbo-Free blocking solution (Vector Laboratories Inc.) for 32 min, followed by a Streptavidin/Biotin Blocking Kit (Vector Laboratories Inc.) with a separate application for 12 min each. We incubated the sections for 4 h (fluorescent) or 1 h (chromogenic) at room temperature (**RT**) with one of the 3 lectins (*Sambucus nigra* lectin [**SNA**], *Maackia amurensis* lectin-I [**MAL-I**], *Maackia amurensis* lectin-II [**MAL-II**]) from Vector Laboratories at the listed concentration in Table 1. For SA α2,6-gal/GalNAc, we incubated slides with biotinylated SNA for both fluorescent and chromogenic staining. A cocktail of fluorescein-labeled MAL-I (specific for N-linked or O-linked glycans with SA α2,3-Galβ (1–4) GlcNAc) and biotinylated MAL-II (specific for O-linked glycans with SA α2,3-Galβ (1–3) GalNAc) was used for fluorescent staining. Biotinylated MAL-I was used separately for chromogenic staining. Following lectin incubation, streptavidin conjugated with Alexa Fluor 594 (Thermo Fisher Scientific) was applied and incubated for 2 h at RT. In the case of chromogenic staining, streptavidin-horseradish peroxidase RTU (Vector Laboratories Inc.) was incubated for 40 min on all 3 biotinylated lectins. We further amplified the chromogenic signal with DISCOVERY Amplification anti-HQ Multimer (Roche Diagnostics Corporation). Fluorescent counterstaining was performed with QD DAPI RUO (Roche Diagnostics Corporation) and mounted manually with Prolong Gold Antifade Mountant without DAPI (Thermo Fisher Scientific). We performed chromogenic counterstaining with hematoxylin and bluing (Roche Diagnostics Corporation) and coverslipping with Sakura Tissue-Tek film. Negative assay controls consisted of primary lectin or antibody omission. We validated positive lectin staining using porcine tissues, as previously established (Nelli et al., 2010). We examined and imaged slides using an Olympus BX-53 trinocular microscope equipped with an Olympus DP23 camera, Excelitas X-Cite mini+ compact illumination system, and CellSyns Dimension software. All tissues were evaluated by multiple American College of Veterinary Pathologists board-certified veterinary pathologists, and results were reported as present or absent using qualitative terms. Tissue staining was not quantified using image software.

Virus Preparation, Inactivation, and Labeling for Virus Histochemistry

A reverse engineered A/bald eagle/Florida/W22-134-OP/2022 (H5N1; rgA/bald eagle/FL/22) that contained

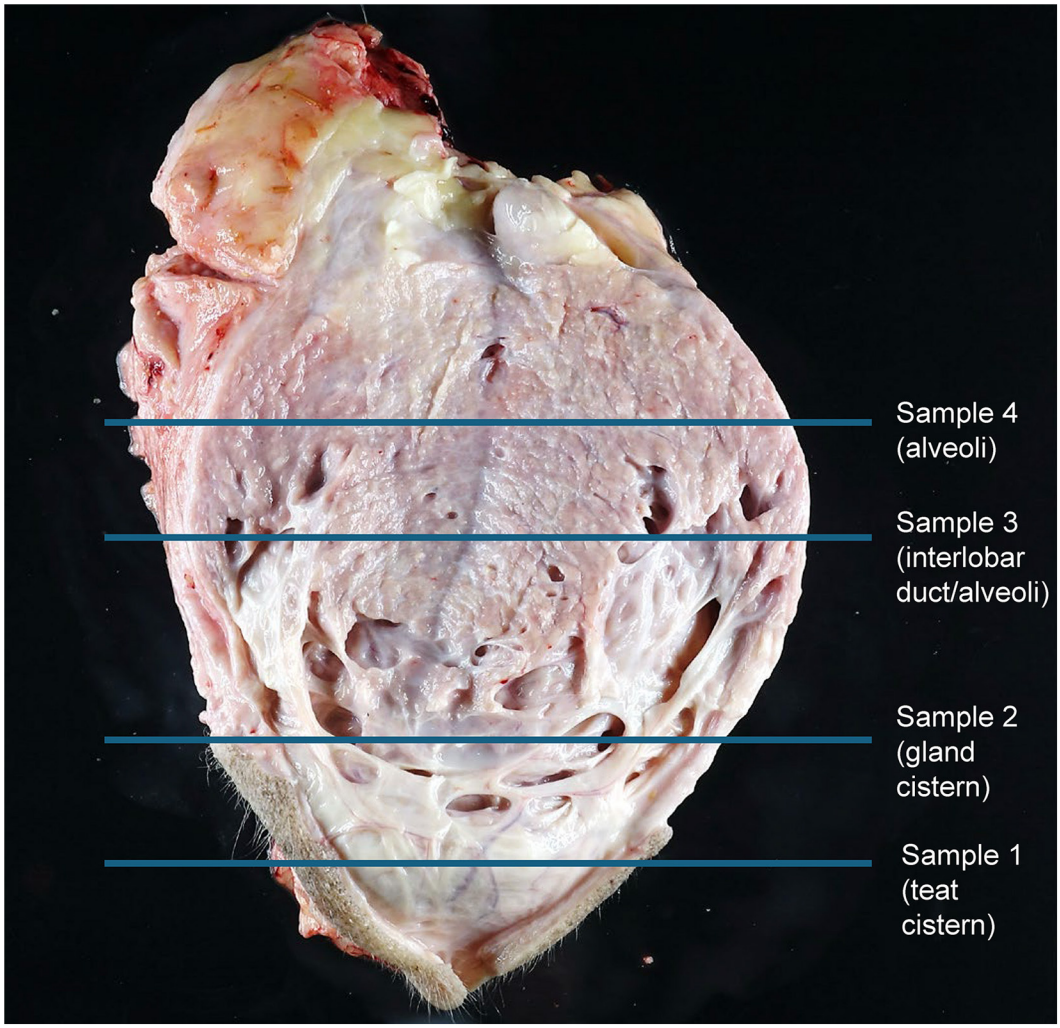

Figure 2. Cross-sectional gross anatomy of the mammary gland of a cow. Lines indicate representative areas where samples were collected for histological studies.

Table 1. Lectin histochemistry and viral binding assay reagents

Item	Conjugate	Working concentration	Manufacturer	Product number
Lectin staining				
Maackia amurensis-I	Fluorescein	20 µg/mL	Vector Laboratories	FL-1311-2
Maackia amurensis-I	Biotinylated	20 µg/mL	Vector Laboratories	B-1315-2
Maackia amurensis-II	Biotinylated	4 µg/mL	Vector Laboratories	B-1265-1
Sambucus nigra	Biotinylated	20 µg/mL	Vector Laboratories	B-1305-2
Streptavidin	Alexa Fluor-594	2 µg/mL	Thermo Fisher Scientific	S11227
Streptavidin	Horseradish peroxidase (HRP) - R.T.U.	1 mg/mL	Vector Laboratories	SA-5704-100
Virus histochemistry				
Fluorescein isothiocyanate isomer (FITC)	None	0.1 mg/mL	Sigma-Aldrich	3326-32-7
Polyclonal rabbit anti-FITC antibody	HRP	20 µg/mL	Agilent Technologies	P5100
Biotin tyramide amplification system	Streptavidin conjugated-HRP	10 µg/mL	Akokya Biosciences	NEL700A001KT
3-amino-9-ethyle-carbazol substrate chromogen	none	Stock	Thermo Fisher Scientific	001122

an engineered low pathogenicity 2.3.4.4b H5 by removal of the polybasic cleavage site, wild type N1, and 6 internal segments from A/Puerto Rico/8/1943 (H1N1) was kindly provided by Richard Webby (St. Jude Children's Research Hospital). We inoculated confluent layers of Madin–Darby canine kidney (**MDCK**) cells with LPAIV H5N1 2.3.4.4b rgA/bald eagle/FL/22. After 48 h, cell culture flasks underwent 2 freeze-thaw cycles at −80°C. After the second cycle, the supernatant was harvested and cleared by low-speed centrifugation. The cleared supernatant was centrifuged at 28,000 rpm in an SW32i rotor at 4°C for 2 h on a layer of 10% sucrose. We resuspended the pellets using PBS buffer and measured for hemagglutination activity (**HA**) by 2-fold serial dilution with turkey red blood cells. The virus was then incubated at RT with an equal volume of 10% neutral buffered formalin for 1 h. We dialyzed the inactivated virus against PBS, confirmed inactivation on MDCK cells, and performed a hemagglutination assay to determine viral titer. The inactivated virus was labeled by mixing with an equal volume of 0.1 mg/mL fluorescein isothiocyanate (**FITC**; Sigma-Aldrich, Saint Louis, MO) in 0.5 *M* bicarbonate buffer (pH 9.5) for 1 h 4°C with constant agitation.

We again dialyzed the labeled virus against PBS and determined the final HA viral titer.

Viral Histochemistry

We performed virus histochemical staining on sections of lactating Holstein dairy cattle and lactating crossbred sows. We deparaffinized the tissues using xylene and rehydrated them through a graded series of alcohol solutions. We applied a 3% hydrogen peroxide solution (Fisher Bioreagents) to quench endogenous peroxidases. We then washed the slides in **TNT** buffer (Tris [Thermo Scientific], sodium chloride solution [Millipore-Sigma, Saint Louis, MO], and Tween20 [Millipore-Sigma]). We immersed the slides in a blocking solution for 1 h at RT (TNT buffer plus blocking reagent, Akoya Biosciences, Marlborough, MA) and incubated the slides overnight at 4°C in a humidified chamber with FITC-labeled rgA/bald eagle/FL/22 (200 HA units per 50 µL). Tissues were then incubated in peroxidase-labeled rabbit anti-FITC antibody (Agilent Technologies, Glostrup, Denmark), followed by signal amplification through a biotin tyramide amplification system (Akoya Biosciences, Marlborough, MA). We visualized peroxidase activity using 3-amino-9-ethylcarbazole (Thermo Fisher Scientific) and counterstained the slides with hematoxylin stain solution (Epredia) and ammonia hydroxide solution (Sigma-Aldrich, St. Louis, MO). For sialidase control, we pre-treated the sow tissue sections with 0.4 U/mL sialidase-A (Agilent Technologies) in 50 m*M* sodium phosphate buffer (pH 6.0) overnight at 37°C and subjected them to the protocol as outlined above. Intestinal tissues from a chicken with and without the FITC-labeled virus were used as positive and negative controls, respectively. We examined and imaged slides using a Olympus BX43 microscope with a DP28 camera and captured photomicrographs using CellSens Standard software.

RESULTS

The results were broadly classified into the teat, gland cistern, interlobular duct, and secretory alveoli regions and summarized in Table 2.

Lectin Labeling in Dairy, Beef, Nonlactating Cattle, Sheep, and Goats

In the ruminants (cattle, sheep, and goats), the epithelial lining of the teat (Figure 3, Ai–Av) and gland cistern (Figure 3, Bi–Bv) showed multifocal to diffuse, moderate positive labeling of SA α2–6 receptors (SNA; Figure 3, Ai–Av, Bi–Bv). This labeling continued into the interlobular duct (Figure 3, Ci–Cv) and secretory alveoli (Figure 3, Di–Dv) with mild to moderate intensity. There was a multifocal labeling of MAL II on the epithelial lining of the teat (Figure 3, Ei–Ev) and gland cistern (Figure 3, Fi–Fv). In the interlobular duct, MAL II labeling was rare, multifocal, and minimal to mild in intensity (Figure 3, Gi–Gv), whereas on the surface of secretory alveoli, the labeling was diffuse and moderate to marked in intensity (Figure 3, Hi–Hv). Interestingly, in nonlactating cattle, the intensity of MAL II labeling was comparatively low from the gland cistern (Figure 3, Fiii), and it continued to be less pronounced in the interlobular duct and secretory alveoli (Figure 3, Giii and Hiii). Overall, the labeling intensity was minimal for MAL II compared with SNA. The spatial distribution of these receptors was apical on the epithelial cell surface and uniform across all animals examined of each species.

Lectin Labeling in Alpacas, Pigs, and Humans

Alpacas showed a similar SNA/MAL II distribution pattern to ruminants. However, the labeling intensity along the epithelial lining of the teat cistern, gland cistern, interlobular ducts, and secretory alveoli (Figure 4, Ai–Di, Ei–Hi) was comparatively more apparent. This labeling on the epithelial lining is multifocal (teat cistern) to diffuse (all other tissues), intense, and apical from the teat cistern to the secretory alveoli.

Both SNA and MAL II labeling was observed in all anatomic regions examined in the closely related monogastric species, pigs and humans. In pigs, the epithelial lining of the teat cistern, gland cistern, interlobular ducts, and secretory alveoli displayed diffuse apical labeling of

Table 2. Sialic acid distribution in the mammary glands of ruminants, monogastric, and pseudoruminant/camelid[1]

Mammary gland region	MAL I (SA α2,3-galβ (1–4) GlcNAc)	MAL II (SA α2,3-galβ (1–3) GalNAc)	SNA (SA α2,6-gal/GalNAc)
Ruminant (goat/sheep/dairy/beef cattle)			
Teat cistern	+ (apical; m/f)	+ (apical; m/f)	+ (apical; d)
Gland cistern	+ (apical; m/f)	+ (apical; m/f)	+ (apical; d)
Interlobular (collecting) duct	+ (apical; * m/f)	+ (apical; * m/f)	+ (apical; d)
Secretory alveoli (glandular epithelium)	+/− (apical; * m/f)	+ (apical;(m/f) * to d)	+ (apical; d)
Nonruminant monogastric (pig/human)			
Teat cistern	+ (apical; m/f)/DNE	+ (apical; d)/DNE	+ (apical; d)/DNE
Gland cistern	+ (apical; m/f)/DNE	+ (apical; d)/DNE	+ (apical; d)/DNE
Interlobular (collecting) duct	+ (apical; m/f)/DNE	+ (apical; d)/ + apical; m/f	+ (apical; d)/+apical; m/f
Secretory alveoli (glandular epithelium)	+/− (apical; m/f)/ + apical; d	+ (apical; d)/+ apical; m/f	+ (apical; d)/+ apical m/f
Pseudoruminant/camelid (alpaca)			
Teat cistern	+ (apical; m/f to d)	+ (apical; m/f)	+ (apical; d)
Gland cistern	+ (apical; m/f to d)	+ (apical; d)	+ (apical; d)
Interlobular (collecting) duct	+ (apical; m/f to d)	+ (apical; d)	+ (apical; d)
Secretory alveoli (glandular epithelium)	+ (apical; m/f to d)	+ (apical; d)	+ (apical; d)

[1]Data representative of n = 3 for all animal species and n = 4 for humans. + denotes positive labeling and − denotes no or minimal labeling; apical means labeling lectins on the epithelial lining; m/f = multifocal labeling; d = diffuse labeling; * denotes nonlactating cattle; DNE = did not examine.

moderate to marked intensity for both SNA and MAL II (Figure 4, Aii–Hii). In humans, the teat and gland cistern are absent; hence, no images were captured (Figure 4, Aiii, Biii, Eiii, and Fiii). However, there was multifocal to diffuse apical epithelial labeling in the interlobular duct and alveoli of moderate intensity for both SNA and MAL II (Figure 4, Ciii and Diii, Giii, and Hiii) in the 4 human specimens tested.

MAL I Lectin Labeling in Ruminants and Nonruminants

The labeling of MAL I, which is specific for N-linked or O-linked glycans with SA α2,3-galβ (1–4) GlcNAc, varied across tissue regions of mammary glands and species evaluated. In the teat and gland cistern of dairy and beef cattle, sheep, and goats, the labeling was multifocal to diffuse and moderately positive compared with occasional positive cells along the epithelial lining in nonlactating dairy cattle (Figure 5, Ai–Av and Bi–Bv). The labeling along the epithelial lining of the interlobular duct and secretory alveoli was weakly positive with occasional focal labeling among all ruminants, again with nonlactating dairy cattle showing poor or no labeling (Figure 5, Ci–Cv and Di–Dv).

In alpacas and pigs, the teat and gland cistern MAL I labeling was multifocal (Figure 5, Ei–Eii and Fi–Fii). Alpacas had multifocal MAL I labeling in interlobular ducts, whereas pigs had continuous apical labeling (Figure 5, Gi and Gii). As in ruminants, MAL I labeling along the epithelial lining of the secretory alveoli was weak or had no labeling in alpacas and pigs (Figure 5, Hi and Hii). Meanwhile, human samples showed continuous apical labeling of MAL I in the alveoli (Figure 5, Hiii).

We further tested all samples using chromogenic labeling to confirm the MAL I labeling because the labeling for MAL I seemed to be less than for SNA and MAL II. Therefore, we wanted an additional assay to confirm our MAL I, IFA findings. In lactating dairy cattle, multifocal labeling was seen in the teat cistern (Figure 6, Ai), with minimal to no apical labeling in other examined areas (Figure 6, Bi–Di). In beef cattle, multifocal to diffuse labeling was used in the teat cistern, gland cistern, and interlobular duct (Figure 6, Aii–Cii). We did not observe labeling in the secretory alveoli (Figure 6m, Dii). In nonlactating cattle, minimal to no labeling was noted across all anatomic locations examined (Figure 6, Aiii–Diii). For sheep and goats, there was multifocal to diffuse labeling in the teat cistern, gland cistern, and interlobular duct (Figure 6m, Aiv–Civ, Av–Cv), but no labeling in the secretory alveoli in either species Figure 6, Div and Dv). We observed multifocal to diffuse labeling for MAL I in alpacas in all examined areas (Figure 6, Ei–Hi). Conversely, pigs only had minimal MAL I labeling in the teat cistern (Figure 6, Eii). The only examined tissue for humans in this case, the interlobular duct, had diffuse apical labeling (Figure 6, Giii).

Virus Histochemistry: Ruminants (Dairy Cattle) and Nonruminants (Pigs)

Viral receptors, as detected by virus histochemistry, were identified at the apical epithelial surface in the interlobular ducts and secretory alveoli of both lactating Holstein cows and cross-bred sows. The distribution of receptors and labeling intensity in the interlobular ducts of lactating Holstein cows varied within individual animals (Figures 7A and 7B). Labeled cells of interlobular ducts commonly had a basilar nucleus and apical cytoplasm. Cells with minimal to no labeling were commonly attenuated or not organized as a stratified cuboidal epi-

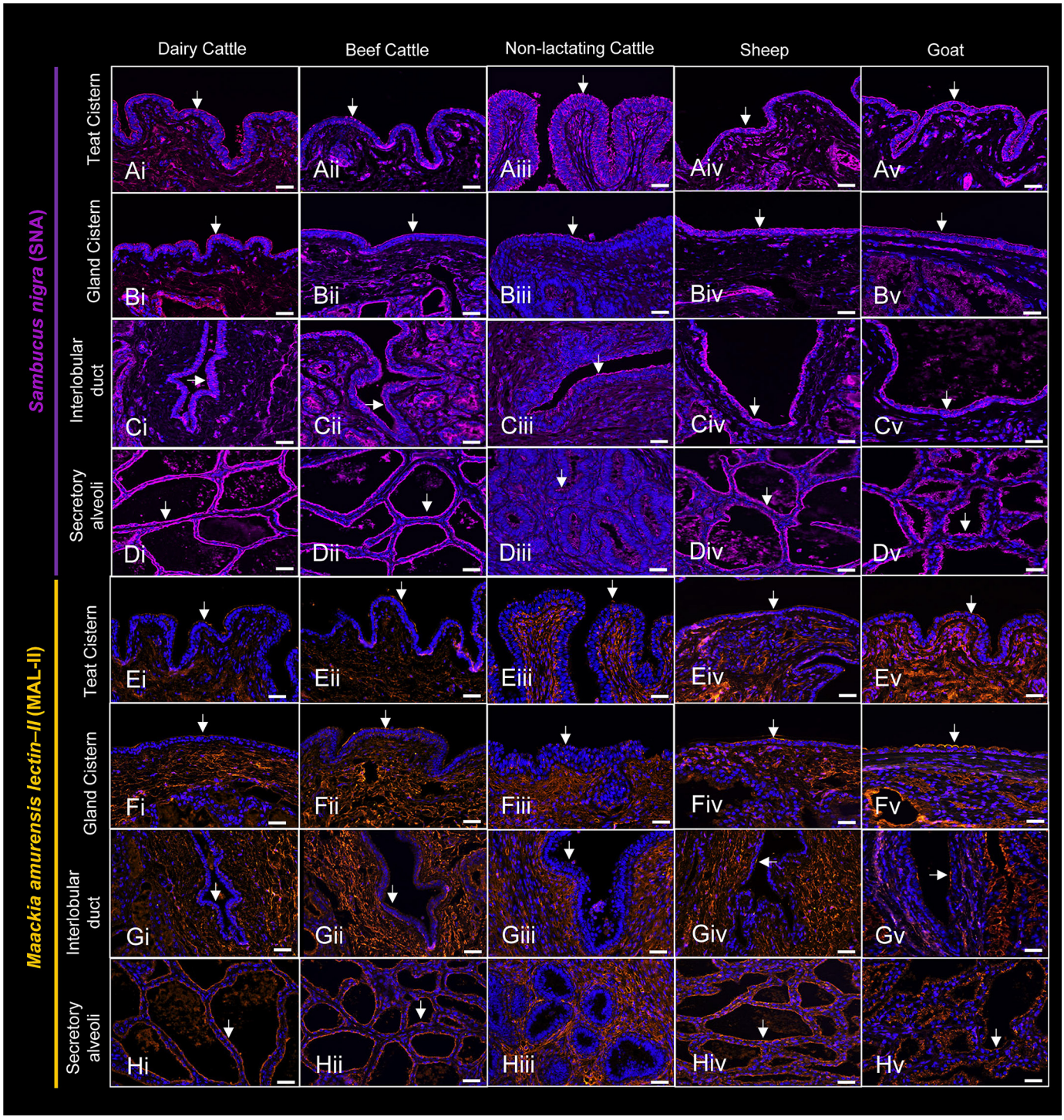

Figure 3. Distribution of sialic acids in the mammary gland of ruminant species. The mammary glands of dairy cattle, beef cattle, nonlactating cattle, sheep, and goats showing *Sambucus nigra* lectin (SNA, purple pseudocolor, Alexa Fluor 594) and *Maackia amurensis* lectin-II (MAL-II, red pseudocolor, Alexa Fluor 594), using fluorescent labeling. The labeling described refers to the epithelial surface of each image. In images Ai–Cv, there is apical, multifocal to diffuse SNA labeling in the teat cistern, gland cistern, and interlobular duct of ruminants. In Di–Dv, there is positive, diffuse, apical labeling for SNA of the epithelial surface of secretory alveoli. In images Ei–Fv, there is multifocal labeling of MAL-II on the epithelial lining of the teat and gland cistern. In Gi–Gv, MAL-II labeling was rare, multifocal, and minimal to mild, except for the nonlactating cow in Giii, which showed minimal appreciable labeling for MAL-II. In Hi–Hv, there was diffuse MAL-II labeling of the epithelial surface of secretory alveoli, again, except for the nonlactating cow in Hiii, which also showed minimal appreciable labeling for MAL-II. However, the apical labeling intensity was lower for MAL-II than for SNA labeling. Arrows indicate the labeling on the epithelial lining. Scale bar = 50 µm.

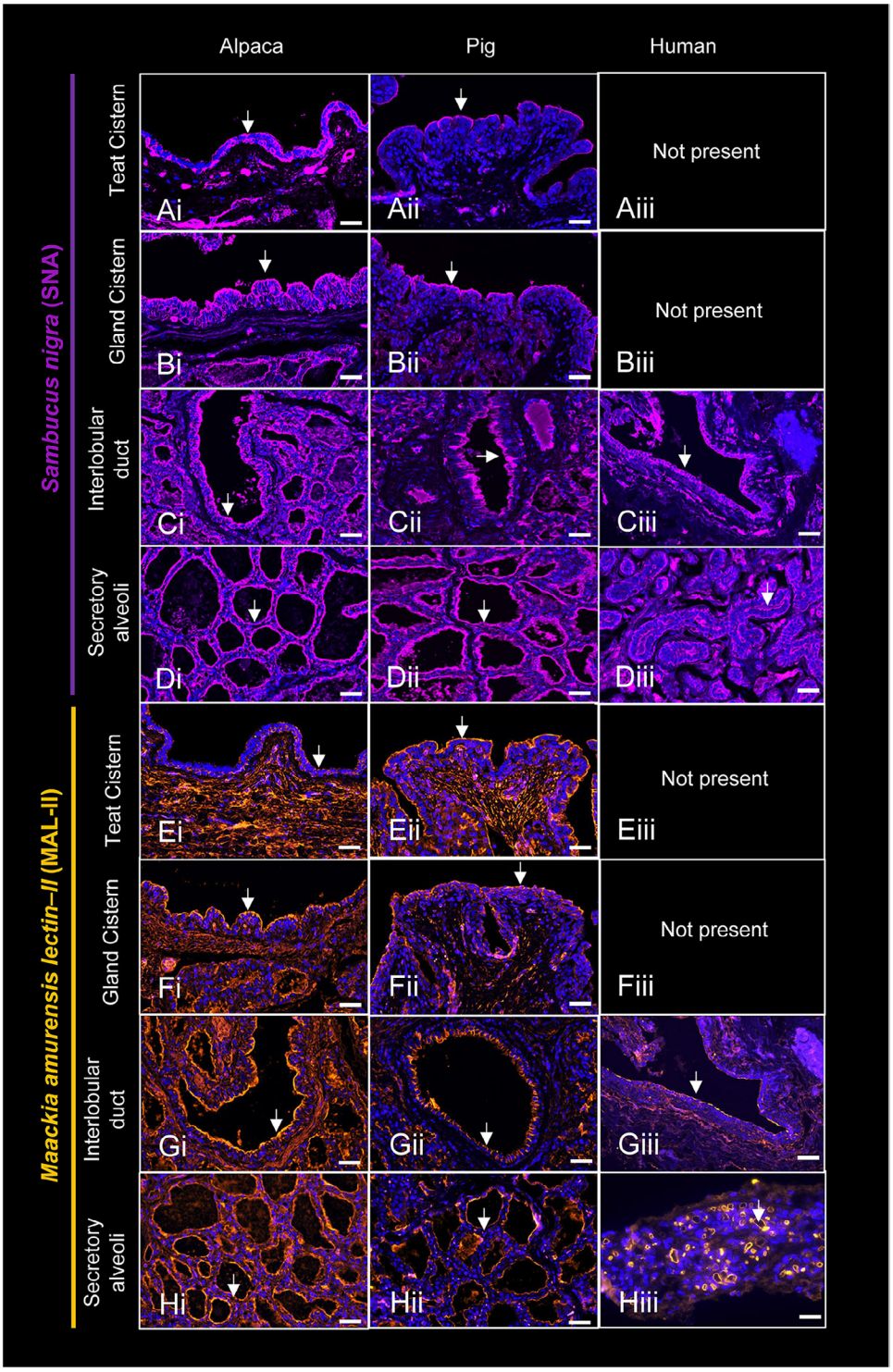

Figure 4. Distribution of sialic acids in the mammary gland of nonruminant species. The mammary glands of alpaca, pig, and human showing *Sambucus nigra* lectin (SNA, purple pseudocolor, Alexa Fluor 594) and *Maackia amurensis* lectin-II (MAL-II, red pseudocolor, Alexa Fluor 594), using fluorescent labeling. Micrographs Ai–Di (alpaca) showed intense diffuse labeling along the epithelial lining of the teat cistern, gland cistern, interlobular duct, and secretory alveoli for SNA. The teat cistern for alpacas showed apical, multifocal, intense labeling for MAL-II (Ei) and diffuse, intense, and apical labeling for MAL-II on the gland cistern, interlobular ducts, and secretory alveoli (Fi, Gi, Hi). In Aii–Hii, images of pigs showed diffuse, apical labeling of moderate to marked intensity for SNA and MAL-II in all anatomic regions examined. Human sections of the interlobular duct and secretory alveoli (Ciii, Diii, Giii, and Hiii) showed multifocal to diffuse apical epithelial labeling for both SNA and MAL-II. Teat and gland cistern are uncommon in the human breast; hence, there are no images, Aiii, Biii, Eiii, and Fiii. Arrows indicate the labeling on the epithelial lining. Scale bar = 50 µm.

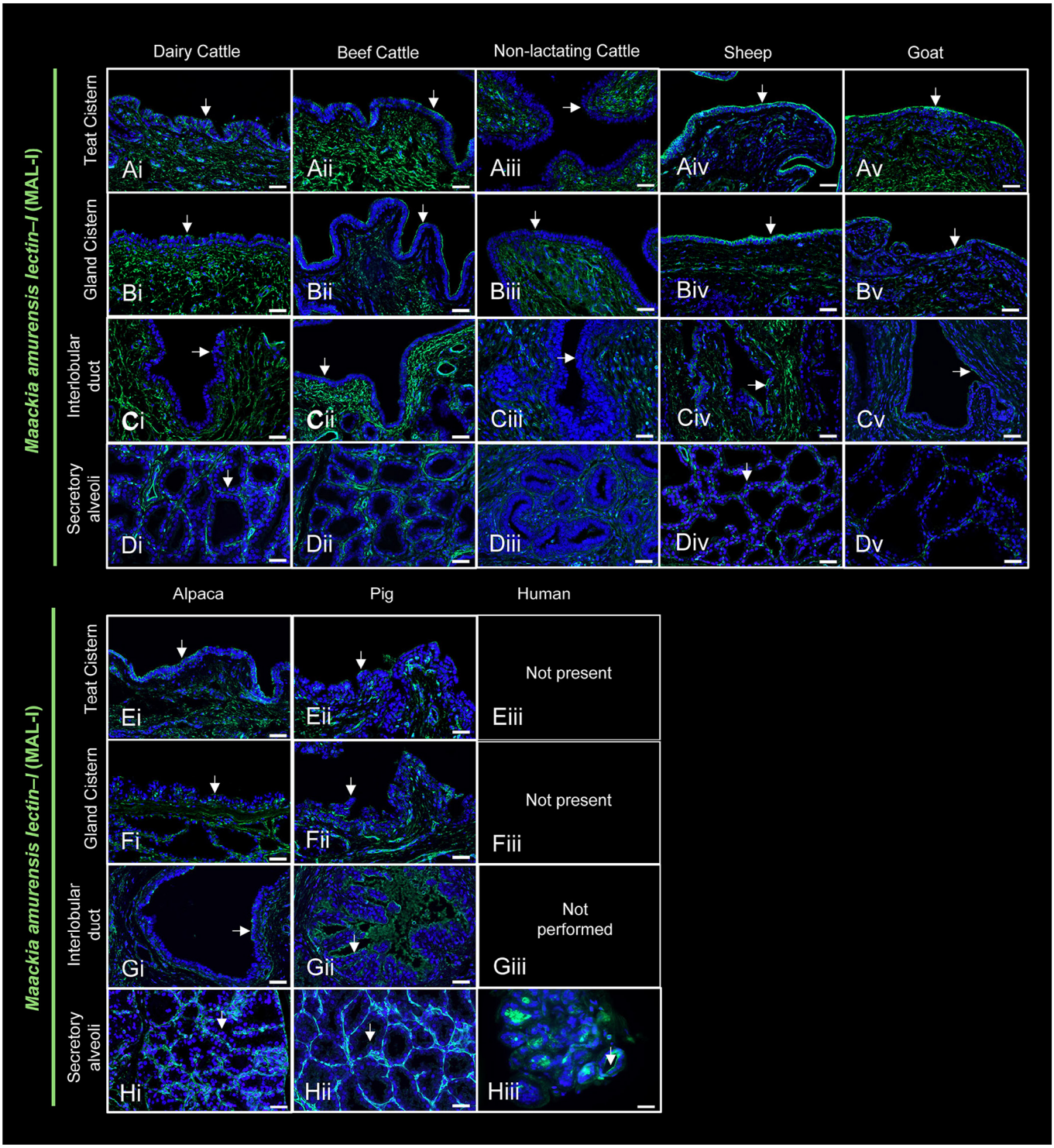

Figure 5. Distribution of sialic acids in the mammary gland of ruminant and nonruminant species, MAL-I specific images using IFA. The mammary glands of dairy cattle, beef cattle, nonlactating cattle, sheep, goats, alpacas, pigs, and humans showing *Maackia amurensis* lectin-I (MAL-I, green pseudocolor, Alexa Fluor 594), using fluorescent labeling. Micrographs Ai–Cv show apical, multifocal MAL-I labeling along the epithelial lining of the teat and gland cistern, as well as the interlobular duct of ruminants. The labeling in the nonlactating cattle teat and gland cistern (Aiii, and Biii) was relatively less pronounced than in other species, including the interlobular duct (Ciii). In the secretory alveoli of all ruminant species (Di-Dv), there is minimal to no apical labeling for MAL-I on the epithelial surface. In Ei–Gii, there is apical, multifocal MAL-I labeling in the teat cistern, gland cistern, and interlobular ducts of alpacas and pigs. In the secretory alveoli of alpacas and pigs (Hi and Hii), there is apical, multifocal, minimal labeling for MAL-I. There is apical, diffuse labeling for MAL-I in human alveoli (Hiii). Arrows indicate the labeling on the epithelial lining. Scale bar = 50 µm.

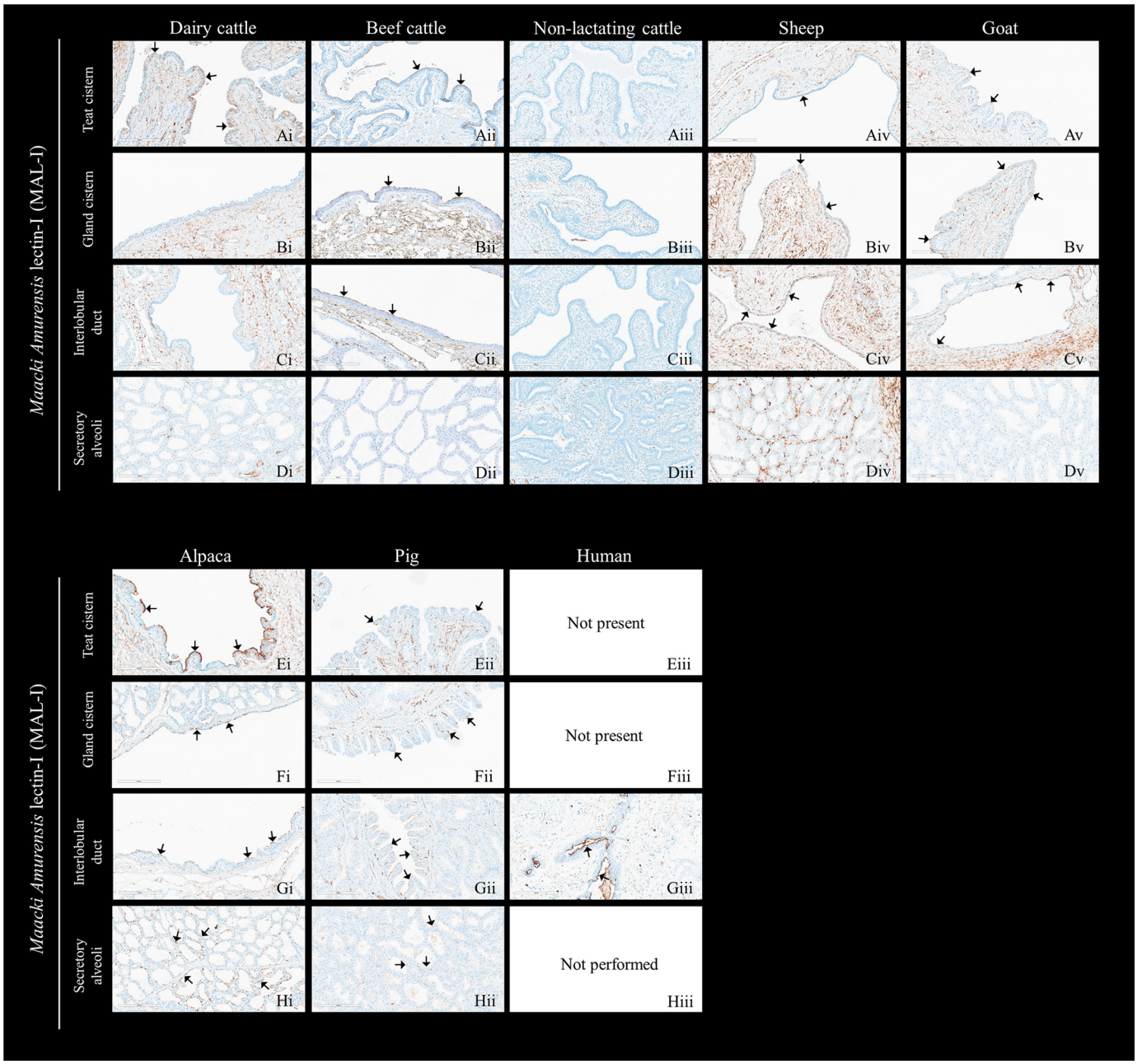

Figure 6. Distribution of sialic acids in the mammary gland of ruminant and nonruminant species, MAL I-specific images using chromogenic staining. The mammary glands of lactating dairy cattle, beef cattle, nonlactating cattle, sheep, and goats with *Maackia amurensis* lectin-I (MAL-I, brown chromogen), using lectin histochemistry. There is a similar multifocal, apical labeling for MAL-I, with no significant apical labeling observed in Aiii, Bi, Biii, Ci, and Ciii. Like As with IFA technique, secretory alveoli had minimal labeling, Di-Dv. Alpaca mammary gland had the most intense apical labeling, with strong apical labeling in the teat cistern, moderate labeling in the gland cistern, scant labeling in the interlobular duct, and moderate labeling within the secretory alveoli (Ei, Fi, Gi, and Hi). The teat cistern of the pig had faint apical labeling (Eii), with no significant labeling in the gland cistern, interlobular duct, or secretory alveoli (Fii, Gii, Hii). Strong apical labeling was present within the interlobular duct of human breast tissue (Giii). Image panel is from one representative animal. Scale bar = 200 µm.

thelial layer (Figure 7A and 7B). Intra-animal variation was also present in secretory alveoli, with some alveoli having circumferential intense labeling adjacent to secretory alveoli with no to minimal labeling, to more consistent labeling of one or more epithelial cells and luminal secretions of adjacent alveoli (Figure 7C and 7D). We commonly identified viral receptors in cross-bred sows on many epithelial cells lining interlobular ducts, one or more epithelial cells lining secretory alveoli, and luminal secretions of adjacent alveoli (Figure 7E and 7F).

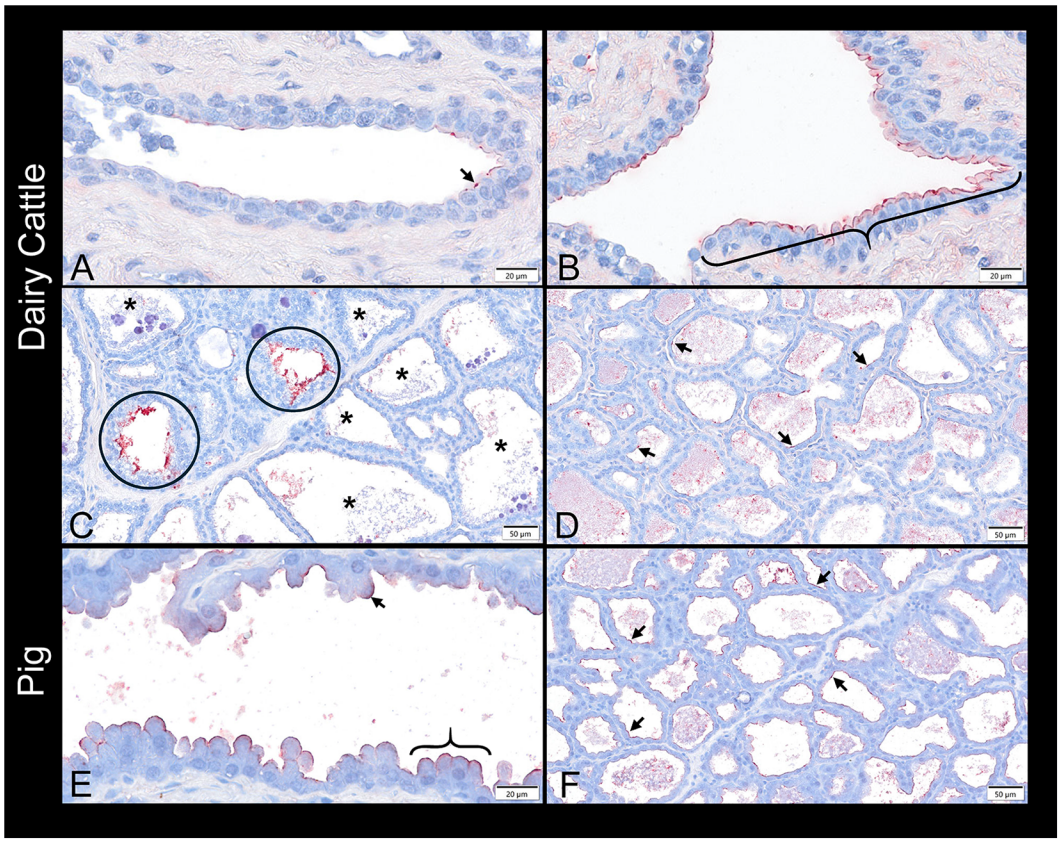

Figure 7. Distribution of LPAIV H5N1 2.3.4.4b rgA/bald eagle/FL/22 2.3.4.4b labeling by virus histochemistry (red) in the mammary gland of lactating Holstein cows and cross-bred sows. Interlobular ducts in the same tissue section of a Holstein dairy cow with minimal labeling (A; arrow) and intense, locally extensive labeling (B; brace). Cells with minimal to no labeling were commonly attenuated (A; arrowhead) or not organized as a stratified cuboidal epithelial layer (B; arrowhead). (C) Nearly circumferential intense labeling of 2 secretory alveoli (circled) adjacent to secretory alveoli with no to minimal labeling of the apical epithelial surface in a Holstein dairy cow (asterisks). (D) More consistent labeling of the apical surface of one or more epithelial cells (arrows) and luminal secretions of adjacent alveoli in a Holstein dairy cow. (E) Interlobular duct of a cross-bred sow with apical labeling of a single epithelial cell (arrow) or row of epithelial cells (brace). (F) Consistent labeling of the apical surface of one or more epithelial cells (arrows) and luminal secretions of adjacent alveoli in a cross-bred sow. Scale bar = 20 µm (A, B, and E); 50 µm (C, D, and F).

Additional viral binding assays revealed positivity in tissues from all examined species, and notable binding was observed on the apical surface of the ducts from alpacas, sheep, goats, and beef cattle (Supplemental Figure S1, see Notes). Human tissue presented sparse staining (Supplemental Figure S1I), but due to the quality and paucity of normal anatomic structures between the neoplastic nodules, an accurate distribution of virus binding was hard to assess. Therefore, future studies will be needed to properly characterize viral binding in human mammary tissue.

DISCUSSION

As HPAI H5N1 continues to enter farms in the United States, infecting several animals and causing human spillover events (CDC, 2025a; USDA, 2025), this study aims to assess the risk of HPAI H5N1 infecting the mammary glands of other domestic species and humans. There is a potential health risk for farm workers, as well as concerns that the virus could appear in other milk-associated products, such as goat milk or cheese, similar to the presence of HPAI H5N1 viral RNA in dairy products (Suarez et al., 2025). In addition, many backyard farms throughout the United States practice mixed animal rearing, and a potential virus entry into these farms may allow for interspecies transmission, as evidenced in Oregon (USDA-APHIS, 2025), with potential to mutate or reassort in these animal species. Influenza A virus infections are well known to affect the respiratory system, and it is the primary site of viral replication and subsequent pathology. But in March of 2024, the detection of HPAI H5N1 in the mammary glands of cows was indeed surprising. Identification of high levels of virus RNA in the milk and the mammary gland epithelial cells of infected dairy cattle suggested the mammary gland as a predilection site for HPAI H5N1 clade 2.3.4.4b replication in this species (Burrough et al., 2024; Nelli et al.,

2024). These observations have been further confirmed through experimental studies (Baker et al., 2025; Halwe et al., 2025). In these challenge studies, cows inoculated with HPAI H5N1 clade 2.3.4.4b viruses in the udder showed viral mastitis with epithelial necrosis within the secretory alveoli. Sequelae included exposure of the basal laminae and myoepithelial cells or replacement of epithelial cells with fibrous connective tissue (Baker et al., 2025; Halwe et al., 2025).

One of the factors contributing to virus attachment and replication is SA, which is abundantly expressed in cow mammary gland epithelium, in particular O-linked glycans with SA α2,3-galβ (1–3) GalNAc, which have more affinity toward IAV of avian origin (Nelli et al., 2024). In response to the current dairy cattle outbreak, the relative abundance of both the avian and mammalian type influenza receptors on the surface of secretory epithelial cells in the mammary glands of dairy cattle most likely allowed for viral binding and entry of HPAI H5N1 2.3.4.4b into this novel anatomic area (Nelli et al., 2024).

Therefore, comparing the spatial distribution of these SA receptors in the mammary glands of ruminants and nonruminant species, including humans, can help assess viral attachment, entry, and risk of replication in this tissue. Pathogens usually gain entry to the mammary gland through the teat canal and spread through the ducts, or they can be systemic and attach to the host cells with appropriate receptors. In this study, we looked at the SA along the epithelial lining of the mammary gland, starting from the teat canal to the lobules, where milk secretion occurs (Figure 1).

Although several studies have looked at the distribution of SA in the respiratory tracts of humans, pigs, cattle, sheep, goats, and camels (Li et al., 2017; Kuchipudi et al., 2021), to our knowledge, this is the first study to compare these receptors in the mammary glands across these species. In alpaca testis and placental epithelial cells, both SA α2,3-gal and SA α2,6-gal were present (Parillo et al., 2009). In addition, SA receptors actively trigger early host immune responses such as cell death signaling (necrosis and apoptosis; Malagolini et al., 2009). Therefore, it is of utmost priority to evaluate the predisposing factors responsible for this new affinity of IAV toward the mammary gland epithelium and the consequences it may have for mammalian species, including humans.

The current study showed that the mammary tissues from ruminants (cattle, sheep, and goat) and nonruminants (alpaca, pig, and human) exhibited labeled SA α2,3-gal and SA α2,6-gal receptors along the mammary epithelium, suggesting that both mammalian and avian IAV have the potential to bind. The SA α2,3-gal spatial distribution identified using MAL-I specific for N-linked or O-linked glycans with SA α2,3-galβ (1–4) GlcNAc and using MAL-II specific for O-linked glycans with SA α2,3-galβ (1–3) GalNAc lectin labeling was particularly interesting because of poor MAL-I labeling along the epithelium (teat and gland cistern) of nonlactating cattle (Figure 5, Aiii and Biii) compared with lactating cattle. A recent study in ex vivo explant cultures of bovine mammary gland tissue showed enhanced HPAI H5N1 (A/dairycattle/Texas/24-008749-001/2024) viral replication in the teat and gland cistern compared with chicken H5N1 belonging to the same 2.3.4.4b clade (Imai et al., 2025). Studies in mice showed selective blocking of SA α2,3-gal associated with MAL-I showed a reduction in viral replication and transmission efficiency in contact mice (Ortigoza et al., 2024). Therefore, it is possible that N-linked or O-linked glycans with SA α2,3-galβ (1–4) GlcNAc (MAL-I) may play an important role in viral attachment and replication. In addition, there is also variability in lectin binding studies in the mammary gland of cattle, both from the studies performed by our team and others (Kristensen et al., 2024; Nelli et al., 2024; Imai et al., 2025). Further infectious and glycan biology studies are needed to confirm the role of MAL-I during HPAI H5N1 viral replication in lactating dairy cattle.

This study also compared the spatial distribution of SAs in human breast tissue and showed the presence of SA α2,3-gal and SA α2,6-gal receptors, which agrees with recent findings (Song et al., 2025). Their study further demonstrated that the proteins from HPAI H5N1 (A/Texas/37/2024) bound to human mammary gland epithelium, but human H1N1 and H3N2 do not bind to this tissue. The potential for HPAI H5N1 to bind to this tissue and possibly replicate could lead to viral mastitis, complications due to unknown etiology, breastfeeding complications, inflammation, pain, and discomfort, compromising both maternal and neonatal health. Hence, there is an immediate urgency to understand the consequences of HPAI H5N1 in human breast tissues.

Using virus histochemistry studies, the LPAIV H5N1 2.3.4.4b rgA/bald eagle/FL/22 was found to be able to bind the apical surface of most interlobular duct epithelium and a subset of epithelial cells lining secretory alveoli. Both structures appeared to have more consistent viral binding in the sow mammary gland than the cow mammary gland, suggesting that although not all cells are similarly susceptible to viral attachment, the sow mammary gland may contain a higher percentage of susceptible cells. The virus binding pattern partially agrees with multifocal labeling of SA α2,3-gal receptors (Table 2; Figures 3, 4, 5, and 6). However, further co-localization studies are required to determine the specificity. Pigs are susceptible to HPAI H5N1 2.3.4.4b virus strains, but whether the virus can successfully travel from the oronasal cavity of the sow or a suckling piglet to the mammary gland is unknown (Arruda et al., 2024). In ferrets, transmission of 2009 H1N1 IAV-inoculated kits to the dam's mammary

gland has occurred (Paquette et al., 2015). The presence of H5 receptors on the sow mammary gland suggests that attachment and replication may also be possible in the sow mammary gland. Endemic swine-adapted H1 and H3 IAV infection is not uncommon in suckling piglets. Nevertheless, associated mastitis in sows has not been documented, either due to the inability of H1 or H3 IAV to cause mastitis, or to a combination of low prevalence, mild disease, or difficulty identifying mastitis because sows are not mechanically milked or routinely evaluated without overt clinical illness. Endemic swine H1 and H3 virus histochemistry on sow mammary tissue is beyond the scope of this study.

Due to facilities and time constraints at the National Animal Disease Center, we attempted to replicate the viral binding assays using the low pathogenic versions of the HA and NA from A/turkey/Minnesota/22-010654-002/2022 (HPAI H5N1 2.3.4.4b clade), which were synthesized and cloned into the reverse genetic plasmid pHW2000 by Twist Biosciences (San Francisco, CA). These 2 plasmids were then combined with reverse genetic plasmids encoding the 6 internal genes of the laboratory-adapted A/Puerto Rico/8/34 (H1N1). The recombinant IAV demonstrated the ability to bind to the apical surface of the interlobular duct epithelium in beef cattle, goats, sheep, alpacas, and humans, as shown by virus histochemistry studies (Supplemental Figure S1). This consistent binding across species correlates with the multifocal distribution of SA α2,3-gal receptors, which are known to mediate attachment of avian-adapted influenza strains. The presence of these receptors in mammary gland tissues suggests that the mammary gland could serve as an alternative replication site for IAV, leading to viral mastitis (Gorden et al., 2025), posing risks to farm workers (CDC, 2025b) and consumers of unpasteurized dairy products (Nooruzzaman et al., 2025).

Although virus histochemistry may provide a more accurate evaluation of the presence and distribution of viral receptors than lectins or recombinant HA proteins, it has limitations. The duration of tissue fixation, tissue autolysis, and the type of fixative may alter results. In this study, livestock tissues were collected shortly after euthanasia and formalin-fixed for less than 48 h. Additionally, the LPAIV H5N1 2.3.4.4b rgA/bald eagle/FL/22 virus was also cultivated in MDCK cells. Although the impact of variable virion shapes and sizes on AIV binding to receptors is not yet completely known, a virus originating from cell culture rather than a clinical specimen could affect virus binding and interpretation (Partlow et al., 2025). In addition, the current study also showed intra-animal variability in the distribution of viral receptors based on virus histochemistry in lactating Holstein dairy cattle, suggesting that not all cells are equally susceptible to viral attachment and, therefore, infection. This variable in susceptibility is also supported by the finding that not all alveoli in inoculated animals are infected or affected by IAV and, at some level, may also contribute to the variability in the clinical disease reported from animals in the field and lesion severity of inoculated animals (Baker et al., 2025).

Manifestation of clinical disease is multifactorial, and although this study evaluated more Holstein dairy cattle than prior publications, it did not actively evaluate Holstein dairy cattle at different stages of lactation or known pathologic conditions, which may contribute to differential glycan expression (Puente and Hueso, 1993; de Sousa et al., 2015). The observation that epithelial cells of probable different maturation vary in labeling by virus histochemistry supports investigating differential glycan expression across different pathologic and physiological states to elucidate host factors that could influence susceptibility.

CONCLUSIONS

Based on these findings, we suggest that IAV have the potential to bind to the mammary glands of cattle, sheep, goats, alpacas, pigs, and humans. Further investigation is needed into the possible sustained IAV replication in the mammary glands of these species, both in experimental and natural environments. Meanwhile, routine milk or milk product testing from these species, together with continued surveillance of the human agricultural interface, will aid in containing the virus spread, establishing mitigation strategies, and understanding evolutionary changes in IAV and their interactions with different species.

NOTES

Financial and programmatic support was provided by the Iowa State University (ISU; Ames, IA) College of Veterinary Medicine through the Mapes Wildlife Care, Education, and Research Endowment, as well as the Iowa Livestock Health Advisory Council. This work was also supported in part by the USDA ARS (project number 5030-32000-231-000-D). Mention of trade names or commercial products in this article is solely for the purpose of providing specific information and does not imply recommendation or endorsement by the US Government. The USDA is an equal opportunity provider and employer. H. S. was supported by an appointment to the USDA-ARS Research Participation Program administered by the Oak Ridge Institute for Science and Education (ORISE) through an interagency agreement between the US Department of Energy (DOE) and the USDA. The Oak Ridge Institute for Science and Education is managed by Oak Ridge Associated Universities

under DOE contract number DE-SC0014664. We are exceedingly grateful to Patrick Halbur, Patrick Gorden, and Rodger Main for their leadership, programmatic support, and guidance, and to the rest of the team in the ISU Veterinary Diagnostic Laboratory and Department of Veterinary Diagnostic and Production Animal Medicine. We are also grateful to Amanda Fales-Williams for her leadership and programmatic support from the ISU Department of Veterinary Pathology, in addition to the help and technical support of Amanda La Coco, Olivia Stewart, Breigha Boyle, Matt Brewer, and Katy Martin, as well as Dean Isaacson from Lab Animal Resources. We also greatly appreciate the guidance, scientific advice, and support we received from Mark Ackermann of the National Animal Disease Center, and the support of Dean Grooms, Jodi McGill, and the research support staff at the College of Veterinary Medicine at ISU. Supplemental material for this article is available at [URL]. The Institutional Animal Care and Use Committee of the ISU College of Veterinary Medicine (Ames, IA; IACUC-24-090) approved this study, and George Mason University (Manassas, VA) provided de-identified, formalin-fixed paraffin-embedded archived breast tissues collected with informed consent and Institutional Review Board approval (GMU IRB# 478170 and 477703). The authors have not stated any conflicts of interest.

Nonstandard abbreviations used: DAPI = xxxxx; FITC = fluorescein isothiocyanate; Gal = galactose; GalNAc = N-acetylgalactosamine; GlcNAc = xxxxx; GMU = George Mason University; HA = hemagglutination activity; HPAI = highly pathogenic avian influenza; IAV = influenza A virus; ISU = Iowa State University; MAL-I = *Maackia amurensis* lectin-I; MAL-II = *Maackia amurensis* lectin-II; MDCK = Madin–Darby canine kidney; RT = room temperature; SA = sialic acid; SNA = *Sambucus nigra* lectin; TNT = Tris, sodium chloride, and Tween20; α2,3-Galβ = α2,3-β-galactose.

REFERENCES

Arnberg, N., K. Edlund, A. H. Kidd, and G. Wadell. 2000. Adenovirus type 37 uses sialic acid as a cellular receptor. J. Virol. 74:42–48. https://doi.org/10.1128/JVI.74.1.42-48.2000.

Arruda, B., A. L. Vincent Baker, A. Buckley, T. K. Anderson, M. Torchetti, N. H. Bergeson, M. L. Killian, and K. Lantz. 2024. Divergent pathogenesis and transmission of highly pathogenic avian influenza A(H5N1) in swine. Emerg. Infect. Dis. 30:738–751. https://doi.org/10.3201/eid3004.231141.

Baker, A. L., B. Arruda, M. V. Palmer, P. Boggiatto, K. Sarlo Davila, A. Buckley, G. Ciacci Zanella, C. A. Snyder, T. K. Anderson, C. R. Hutter, T. Q. Nguyen, A. Markin, K. Lantz, E. A. Posey, M. Kim Torchetti, S. Robbe-Austerman, D. R. Magstadt, and P. J. Gorden. 2025. Dairy cows inoculated with highly pathogenic avian influenza virus H5N1. Nature 637:913–920. https://doi.org/10.1038/s41586-024-08166-6.

Burrough, E. R., D. R. Magstadt, B. Petersen, S. J. Timmermans, P. C. Gauger, J. Zhang, C. Siepker, M. Mainenti, G. Li, A. C. Thompson, P. J. Gorden, P. J. Plummer, and R. Main. 2024. Highly pathogenic avian influenza A(H5N1) clade 2.3.4.4b virus infection in domestic dairy cattle and cats, United States, 2024. Emerg. Infect. Dis. 30:1335–1343. https://doi.org/10.3201/eid3007.240508.

Cavalcante, T., M. M. Medeiros, S. N. Mule, G. Palmisano, and B. S. Stolf. 2021. The role of sialic acids in the establishment of infections by pathogens, with special focus on *Leishmania*. Front. Cell. Infect. Microbiol. 11:671913. https://doi.org/10.3389/fcimb.2021.671913.

CDC (Centers for Disease Control and Prevention). 2025a. H5 Bird Flu: Current Situation. Accessed Jan. 27, 2025. https://www.cdc.gov/bird-flu/situation-summary/index.html.

CDC. (Centers for Disease Control and Prevention). 2025b. Information for Workers Exposed to H5N1 Bird Flu. Accessed Oct. 23, 2025. https://www.cdc.gov/bird-flu/worker-safety/farm-workers.html.

CDC. (Centers for Disease Control and Prevention). 2025c. Past Reported Global Human Cases with Highly Pathogenic Avian Influenza A. (H5N1) (HPAI H5N1) by Country, 1997–2024. Accessed January 4, 2025. https://www.cdc.gov/bird-flu/php/avian-flu-summary/chart-epi-curve-ah5n1.html.

de Sousa, Y. R. F., M. A. da Silva Vasconcelos, R. G. Costa, C. A. de Azevedo Filho, E. P. de Paiva, and R. C. R. E. Queiroga. 2015. Sialic acid content of goat milk during lactation. Livest. Sci. 177:175–180. https://doi.org/10.1016/j.livsci.2015.04.005.

Eneva, R., S. Engibarov, R. Abrashev, E. Krumova, and M. Angelova. 2021. Sialic acids, sialoconjugates and enzymes of their metabolism in fungi. Biotechnol. Biotechnol. Equip. 35:346–357. https://doi.org/10.1080/13102818.2021.1879678.

Ghosh, S. 2020. Sialic acid and biology of life: An introduction. Pages 1–61 in Sialic Acids and Sialoglycoconjugates in the Biology of Life, Health and Disease. Elsevier.

Gorden, P. J., D. R. Magstadt, A. L. Baker, B. L. Arruda, T. M. Bell, and R. K. Nelli. 2025. Viral mastitis associated with influenza A in dairy cattle. Vet. Clin. North Am. Food Anim. Pract. 41:271–283. https://doi.org/10.1016/j.cvfa.2025.02.010.

Halwe, N. J., K. Cool, A. Breithaupt, J. Schön, J. D. Trujillo, M. Nooruzzaman, T. Kwon, A. K. Ahrens, T. Britzke, C. D. McDowell, R. Piesche, G. Singh, V. Pinho dos Reis, S. Kafle, A. Pohlmann, N. N. Gaudreault, B. Corleis, F. M. Ferreyra, M. Carossino, U. B. R. Balasuriya, L. Hensley, I. Morozov, L. M. Covaleda, D. Diel, L. Ulrich, D. Hoffmann, M. Beer, and J. A. Richt. 2025. H5N1 clade 2.3.4.4b dynamics in experimentally infected calves and cows. Nature 637:903–912. https://doi.org/10.1038/s41586-024-08063-y.

Haselhorst, T., F. E. Fleming, J. C. Dyason, R. D. Hartnell, X. Yu, G. Holloway, K. Santegoets, M. J. Kiefel, H. Blanchard, B. S. Coulson, and M. Von Itzstein. 2009. Sialic acid dependence in rotavirus host cell invasion. Nat. Chem. Biol. 5:91–93. https://doi.org/10.1038/nchembio.134.

Haxhiaj, K., D. S. Wishart, and B. N. Ametaj. 2022. Mastitis: What it is, current diagnostics, and the potential of metabolomics to identify new predictive biomarkers. Dairy 3:722–746. https://doi.org/10.3390/dairy3040050.

Hopkins, A. P., J. A. Hawkhead, and G. H. Thomas. 2013. Transport and catabolism of the sialic acids N-glycolylneuraminic acid and 3-keto-3-deoxy-d-glycero-d-galactonononic acid by *Escherichia coli* K-12. FEMS Microbiol. Lett. 347:14–22. https://doi.org/10.1111/1574-6968.12213.

Huang, L.-Y., A. Patel, R. Ng, E. B. Miller, S. Halder, R. McKenna, A. Asokan, and M. Agbandje-McKenna. 2016. Characterization of the adeno-associated virus 1 and 6 sialic acid binding site. J. Virol. 90:5219–5230. https://doi.org/10.1128/JVI.00161-16.

Imai, M., H. Ueki, M. Ito, K. Iwatsuki-Horimoto, M. Kiso, A. Biswas, S. Trifkovic, N. Cook, P. J. Halfmann, G. Neumann, A. J. Eisfeld, and Y. Kawaoka. 2025. Highly pathogenic avian H5N1 influenza A virus replication in ex vivo cultures of bovine mammary gland and teat tissues. Emerg. Microbes Infect. 14:2450029. https://doi.org/10.1080/22221751.2025.2450029.

Kristensen, C., L. E. Larsen, R. Trebbien, and H. E. Jensen. 2024. The avian influenza A virus receptor SA-α2,3-Gal is expressed in the porcine nasal mucosa sustaining the pig as a mixing vessel for new influenza viruses. Virus Res. 340:199304. https://doi.org/10.1016/j.virusres.2023.199304.

Kuchipudi, S. V., R. K. Nelli, A. Gontu, R. Satyakumar, M. Surendran Nair, and M. Subbiah. 2021. Sialic acid receptors: The key to solving the enigma of zoonotic virus spillover. Viruses 13:262. https://doi.org/10.3390/v13020262.

Le, T. V., L. T. Phan, K. H. K. Ly, L. T. Nguyen, H. T. Nguyen, N. T. T. Ho, T. X. Trinh, and N. N. Tran Minhh. 2019. Fatal avian influenza A(H5N1) infection in a 36-week pregnant woman survived by her newborn in Sóc Trăng Province, Vietnam, 2012. Influenza Other Respir. Viruses 13:292–297. https://doi.org/10.1111/irv.12614.

Lewis, A. L., X. Chen, R. L. Schnaar, and A. Varki. 2022. Sialic acids and other nonulosonic acids. Pages in Essentials of Glycobiology. 3rd ed. A. Varki, R. D. Cummings, J. D. Esko, P. Stanley, G. W. Hart, M. Aebi, A. G. Darvill, T. Kinoshita, N. H. Packer, J. H. Prestegard, R. L. Schnaar, and P. H. Seeberger, ed. Cold Spring Harbor Laboratory Press.

Li, W., R. J. G. Hulswit, I. Widjaja, V. S. Raj, R. McBride, W. Peng, W. Widagdo, M. A. Tortorici, B. Van Dieren, Y. Lang, J. W. M. Van Lent, J. C. Paulson, C. A. M. De Haan, R. J. De Groot, F. J. M. Van Kuppeveld, B. L. Haagmans, and B. J. Bosch. 2017. Identification of sialic acid-binding function for the Middle East respiratory syndrome coronavirus spike glycoprotein. Proc. Natl. Acad. Sci. USA 114:E8508–E8517. https://doi.org/10.1073/pnas.1712592114.

Malagolini, N., M. Chiricolo, M. Marini, and F. Dall'Olio. 2009. Exposure of α2,6-sialylated lactosaminic chains marks apoptotic and necrotic death in different cell types. Glycobiology 19:172–181. https://doi.org/10.1093/glycob/cwn122.

Matrosovich, M., G. Herrler, and H. D. Klenk. 2013. Sialic acid receptors of viruses. Pages 1–28 in SialoGlyco Chemistry and Biology II. R. Gerardy-Schahn, P. Delannoy, and M. Von Itzstein, ed. Springer International Publishing.

Matrosovich, M., N. Zhou, Y. Kawaoka, and R. Webster. 1999. The surface glycoproteins of H5 influenza viruses isolated from humans, chickens, and wild aquatic birds have distinguishable properties. J. Virol. 73:1146–1155. https://doi.org/10.1128/JVI.73.2.1146-1155.1999.

Mellis, A. M., J. Coyle, K. E. Marshall, A. M. Frutos, J. Singleton, C. Drehoff, A. Merced-Morales, H. P. Pagano, R. O. Alade, E. B. White, E. K. Noble, C. Holiday, F. Liu, S. Jefferson, Z.-N. Li, F. L. Gross, S. J. Olsen, V. G. Dugan, C. Reed, S. Ellington, S. Montoya, A. Kohnen, G. Stringer, N. Alden, P. Blank, D. Chia, N. Bagdasarian, R. Herlihy, S. Lyon-Callo, and M. Z. Levine. 2024. Serologic evidence of recent infection with highly pathogenic avian influenza A(H5) virus among dairy workers—Michigan and Colorado, June–August 2024. MMWR Morb. Mortal. Wkly. Rep. 73:1004–1009. https://doi.org/10.15585/mmwr.mm7344a3.

Naguib, M. M., P. Eriksson, E. Jax, M. Wille, C. Lindskog, C. Bröjer, J. Krambrich, J. Waldenström, R. H. S. Kraus, G. Larson, Å. Lundkvist, B. Olsen, J. D. Järhult, and P. Ellström. 2023. A comparison of host responses to infection with wild-type avian influenza viruses in chickens and tufted ducks. Microbiol. Spectr. 11:e02586-22. https://doi.org/10.1128/spectrum.02586-22.

Nelli, R. K., T. A. Harm, C. Siepker, J. M. Groeltz-Thrush, B. Jones, N. C. Twu, A. S. Nenninger, D. R. Magstadt, E. R. Burrough, P. E. Piñeyro, M. Mainenti, S. Carnaccini, P. J. Plummer, and T. M. Bell. 2024. Sialic acid receptor specificity in mammary gland of dairy cattle infected with highly pathogenic avian influenza A(H5N1) virus. Emerg. Infect. Dis. 30:1361–1373. https://doi.org/10.3201/eid3007.240689.

Nelli, R. K., S. V. Kuchipudi, G. A. White, B. B. Perez, S. P. Dunham, and K.-C. Chang. 2010. Comparative distribution of human and avian type sialic acid influenza receptors in the pig. BMC Vet. Res. 6:4. https://doi.org/10.1186/1746-6148-6-4.

Nguyen, L., K. A. McCord, D. T. Bui, K. M. Bouwman, E. N. Kitova, M. Elaish, D. Kumawat, G. C. Daskhan, I. Tomris, L. Han, P. Chopra, T. J. Yang, S. D. Willows, A. L. Mason, L. K. Mahal, T. L. Lowary, L. J. West, S. T. D. Hsu, T. Hobman, S. M. Tompkins, G. J. Boons, R. P. de Vries, M. S. Macauley, and J. S. Klassen. 2022. Sialic acid-containing glycolipids mediate binding and viral entry of SARS-CoV-2. Nat. Chem. Biol. 18:81–90. https://doi.org/10.1038/s41589-021-00924-1.

Nooruzzaman, M., P. S. B. de Oliveira, S. L. Butt, N. H. Martin, S. D. Alcaine, S. P. Walker, and D. G. Diel. 2025. H5N1 influenza virus stability and transmission risk in raw milk and cheese. Nat. Med. 2025:1–9. https://doi.org/10.1038/s41591-025-04010-0.

O'Hara, S. D., T. Stehle, and R. Garcea. 2014. Glycan receptors of the Polyomaviridae: Structure, function, and pathogenesis. Curr. Opin. Virol. 7:73–78. https://doi.org/10.1016/j.coviro.2014.05.004.

Ortigoza, M. B., C. L. Mobini, H. L. Rocha, S. Bartlett, C. A. Loomis, and J. N. Weiser. 2024. Inhibiting influenza virus transmission using a broadly acting neuraminidase that targets host sialic acids in the upper respiratory tract. MBio 15:e02203-23. https://doi.org/10.1128/mbio.02203-23.

Paquette, S. G., D. Banner, S. S. H. Huang, R. Almansa, A. Leon, L. Xu, J. Bartoszko, D. J. Kelvin, and A. A. Kelvin. 2015. Influenza transmission in the mother-infant dyad leads to severe disease, mammary gland infection, and pathogenesis by regulating host responses. PLoS Pathog. 11:e1005173. https://doi.org/10.1371/journal.ppat.1005173.

Parillo, F., G. E. Magi, S. Diverio, and G. Catone. 2009. Immunohistochemical and lectin histochemical analysis of the alpaca efferent ducts. Histol. Histopathol. 24:1–12. https://doi.org/10.14670/HH-24.1.

Partlow, E. A., A. Jaeggi-Wong, S. D. Planitzer, N. Berg, Z. Li, and T. Ivanovic. 2025. Influenza A virus rapidly adapts particle shape to environmental pressures. Nat. Microbiol. 10:784–794. https://doi.org/10.1038/s41564-025-01925-9.

Puente, R., and P. Hueso. 1993. Lactational changes in the N-glycoloylneuraminic acid content of bovine milk gangliosides. Biol. Chem. Hoppe Seyler 374:475–478. https://doi.org/10.1515/bchm3.1993.374.7-12.475.

Rifatbegović, M., R. A. J. Nicholas, T. Mutevelić, M. Hadžiomerović, and Z. Maksimović. 2024. Pathogens associated with bovine mastitis: The experience of Bosnia and Herzegovina. Vet. Sci. 11:63. https://doi.org/10.3390/vetsci11020063.

Sharma, R., S. Ahlawat, H. Sharma, R. A. K. Aggarwal, V. Sharma, and M. S. Tantia. 2019. Variable sialic acid content in milk of Indian cattle and buffalo across different stages of lactation. J. Dairy Res. 86:98–101. https://doi.org/10.1017/S002202991800081X.

Shu, Y., H. Yu, and D. Li. 2006. Lethal avian influenza A (H5N1) infection in a pregnant woman in Anhui Province, China. N. Engl. J. Med. 354:1421–1422. https://doi.org/10.1056/NEJMc053524.

Song, H., T. Hao, P. Han, H. Wang, X. Zhang, X. Li, Y. Wang, J. Chen, Y. Li, X. Jin, X. Duan, W. Zhang, Y. Bi, R. Jin, L. Sun, N. Wang, and G. F. Gao. 2025. Receptor binding, structure, and tissue tropism of cattle-infecting H5N1 avian influenza virus hemagglutinin. Cell 188:919–929.e9. https://doi.org/10.1016/j.cell.2025.01.019.

Stuart, A. D., and T. D. K. Brown. 2007. α2,6-Linked sialic acid acts as a receptor for feline calicivirus. J. Gen. Virol. 88:177–186. https://doi.org/10.1099/vir.0.82158-0.

Suarez, D. L., I. V. Goraichuk, L. Killmaster, E. Spackman, N. J. Clausen, T. J. Colonius, C. L. Leonard, and M. L. Metz. 2025. Testing of retail cheese, butter, ice cream, and other dairy products for highly pathogenic avian influenza in the US. J. Food Prot. 88:100431. https://doi.org/10.1016/j.jfp.2024.100431.

Tan, C. W., C. H. Huan Hor, S. S. Kwek, H. K. Tee, I. C. Sam, E. L. K. Goh, E. E. Ooi, Y. F. Chan, and L. F. Wang. 2019. Cell surface α2,3-linked sialic acid facilitates Zika virus internalization. Emerg. Microbes Infect. 8:426–437. https://doi.org/10.1080/22221751.2019.1590130.

Taube, S., J. W. Perry, K. Yetming, S. P. Patel, H. Auble, L. Shu, H. F. Nawar, C. H. Lee, T. D. Connell, J. A. Shayman, and C. E. Wobus. 2009. Ganglioside-linked terminal sialic acid moieties on murine macrophages function as attachment receptors for murine noroviruses. J. Virol. 83:4092–4101. https://doi.org/10.1128/JVI.02245-08.

Teoh, S. T., M. P. Ogrodzinski, C. Ross, K. W. Hunter, and S. Y. Lunt. 2018. Sialic acid metabolism: A key player in breast cancer metastasis revealed by metabolomics. Front. Oncol. 8:174. https://doi.org/10.3389/fonc.2018.00174.

Tran, T. H., T. L. Nguyen, T. D. Nguyen, T. S. Luong, P. M. Pham, V. V. C. Nguyen, and T. S. Pham. C. D. Vo, T. Q. M. Le, T. T. Ngo, B. K. Dao, P. P. Le, T. T. Nguyen, T. L. Hoang, V. T. Cao, T. G. Le, D. T. Nguyen, H. N. Le, K. T. Nguyen, H. S. Le, V. T. Le, D. Christiane,

T. T. Tran, D. J. Menno, C. Schultz, P. Cheng, W. Lim, P. Horby, J. Farrar, and World Health Organization International Avian Influenza Investigative Team. 2004. Avian influenza A (H5N1) in 10 patients in Vietnam. N. Engl. J. Med. 350:1179–1188. https://doi.org/10.1056/NEJMoa040419.

Uiprasertkul, M., P. Puthavathana, K. Sangsiriwut, P. Pooruk, K. Srisook, M. Peiris, J. M. Nicholls, K. Chokephaibulkit, N. Vanprapar, and P. Auewarakul. 2005. Influenza A H5N1 replication sites in humans. Emerg. Infect. Dis. 11:1036–1041. https://doi.org/10.3201/eid1107.041313.

USDA. 2025. H5N1 Influenza. Accessed Oct. 25, 2025. https://www.aphis.usda.gov/h5n1-hpai#detections-hpai.

USDA-APHIS. 2025. USDA Animal and Plant Health Inspection Service Shares Update on H5N1 Detection in Oregon Swine, Bovine Vaccine Candidate Progression. Accessed Oct. 25, 2025. https://www.aphis.usda.gov/news/agency-announcements/usda-animal-plant-health-inspection-service-shares-update-h5n1-detection.

USDA-APHIS Wildlife Services. 2025. HPAI Detections in Mammals. Accessed Mar. 13, 2025. https://www.aphis.usda.gov/livestock-poultry-disease/avian/avian-influenza/hpai-detections/mammals.

Wang, B., and J. Brand-Miller. 2003. The role and potential of sialic acid in human nutrition. European Journal of Clinical Nutrition 2003 57:11 57:1351–1369. https://doi.org/10.1038/sj.ejcn.1601704.

Warwas, M. L., J. N. Watson, A. J. Bennet, and M. M. Moore. 2007. Structure and role of sialic acids on the surface of Aspergillus fumigatus conidiospores. Glycobiology 17:401–410. https://doi.org/10.1093/glycob/cwl085.

WHO (World Health Organization). 2024. Cumulative number of confirmed human cases for avian influenza A(H5N1) reported to WHO, 2003–2024, 1 November 2024.

Wieland, M. 2024. Mastitis in Cattle. Accessed Sep. 11, 2025. https://www.merckvetmanual.com/reproductive-system/mastitis-in-large-animals/mastitis-in-cattle.

Zhang, Y., W. Liu, F. He, Y. J. Liu, H. Jiang, C. Hao, and W. Wang. 2024. Myosin 9 and N-glycans jointly regulate human papillomavirus entry. J. Biol. Chem. 300:105660. https://doi.org/10.1016/j.jbc.2024.105660.

Zhao, C., X. Hu, M. Qiu, L. Bao, K. Wu, X. Meng, Y. Zhao, L. Feng, S. Duan, Y. He, N. Zhang, and Y. Fu. 2023. Sialic acid exacerbates gut dysbiosis-associated mastitis through the microbiota-gut-mammary axis by fueling gut microbiota disruption. Microbiome 11:78. https://doi.org/10.1186/s40168-023-01528-8.

ORCIDS

Rahul K. Nelli, https://orcid.org/0000-0001-8765-0943
Olufemi Fasina, https://orcid.org/0000-0003-3893-5234
Rachel Phillips, https://orcid.org/0009-0009-7545-1483
Brianna Jones, https://orcid.org/0009-0003-0915-5770
Virginia Espina, https://orcid.org/0000-0001-5080-5972
Hannah Seger, https://orcid.org/0000-0001-7693-2232
Manoj Kumar, https://orcid.org/0000-0003-0312-0676
Qamar Ul Hassan, https://orcid.org/0009-0005-3075-9258
Gulnara Brixius, https://orcid.org/0000-0001-7721-2720
C. Joaquin Caceres, https://orcid.org/0000-0001-8508-6592
Todd M. Bell https://orcid.org/0009-0007-6420-3367